A tracing method of landslides sediment embedded in CAESAR-Lisflood landscape evolution model

Jun Xie [a, b], Tom J Coulthard [a, b]

[a] Energy and Environment Institute, University of Hull, Hull, UK

[b] Department of Geography, Geology and Environment, University of Hull, Hull, UK

Abstract: Quantifying the amount of landslide related sediment budget and time-scale of the long-term legacy of seismic landslides is crucial to understand the landslides impact on the sediment dynamics and landform changes. However, the quantification of landslide-sourced sediment dynamics and routing remains was an open question. In this study, a number of modifications are made to the CAESAR-Lisflood (CL) which integrated with a tracing function after landslides triggering with spatially variable slope threshold. First, an approach using a spatially variable slope threshold was firstly applied in CL to trigger landslides with pre-defined threshold slope angle. The CL model was further modified based on previous version to enable the spatial input of sediment grain size distribution (GSD), which allow the model to distinguish the grain size composition of landslides sediment and the background sediment sourced from other area. Further, a modified version of CL model was firstly developed with a tracing function integrated to track the landslide-sourced sediment transport and routing. The simulation results show that the modified CL can generate not only the spatial pattern but also the vertical extent of sediment transport from each sourced area. The model can also output the sediment yield at the basin outlet from different sourced areas at user specified time interval. This enable us to investigate the landslide-generated sediment dynamics and its impact on landscape evolution over a broad scales of time and space.

1. Introduction

A wide range of landscape evolution modelling approaches have been developed focusing on the interactions between fluvial, hydrology and slope process (Veldkamp and Van Dijke, 2000; Tucker et al., 2001; García-Castellanos et al., 2012; Coulthard et al., 2013b; Armitage et al., 2015). These landscape models use different numerical modelling approaches according to the focus of modelling scope and different spatial-temporal scales of their application. Meadows (2014) appraised a series of landscape evolution models (LEMs) based on the multi-process representation including hydrodynamic, fluvial and sediment transport processes, and he concluded that the CL model have the most comprehensive performance in terms of multi-process representation including sediment heterogeneity (e.g. multiple active layers and grain sizes). Given LEM's have the ability to simulate the interaction of several different geomorphic processes – they may be useful for studying how landslides affect basin sediment fluxes and landscape evolution.

The contribution and complete role of landslides to landscape evolution has recently attracted more attention (Cendrero and Dramis, 1996; Korup, 2009; Korup et al., 2010), which give rise to the resurgence of landscape evolution numerical models that incorporate the impact of landslides (Densmore et al., 1998; Claessens et al., 2006). In some of these numerical models, landslide triggering can be modelled via a threshold slope angle or a critical hillslope height at which landslides will occur (Korup et al., 2007). The removing process of mass movement in slope is complicated and multi-process models which consider landslides processes typically determine a critical slope angle, below which sediment is transported by diffusion, and above which, sediment is transported by slope-clearing process until the slope gradient reduces to a threshold angle (Kirkby, 1984). Additionally, there are been a range of mathematical and conceptual models simulating slope evolution, incorporating the effects of landslides (Cendrero and Dramis, 1996), describing the "how" but do not "how much" landslides are contributing to landscape evolution (Cendrero and Dramis, 1996). Transport laws for mass movement including shallow and deep landslides, rockfall, rotational slides are more sophisticated. Two general approaches are commonly applied to tackle relatively shallow, rapid landslides in landscape evolution models: flux-based methods and event-based methods (Tucker and Hancock, 2010). However, to date, deep seated landslides have not been elaborately considered in landscape evolution models.

An alternative approach is to explicitly predict the occurring of individual landslides events and track their motion across topography.For example, Claessens et al. (2006) reconstructed the incidence of landslide episodes in a catchment using landslides integrated LAPSUS landscape evolution model. A Lagrangian method was introduced to consider bedrock landslides in the ZSCAPE model which applies a stochastic triggering algorithm (Densmore et al., 1998), and van der Beek and Braun used a similar method to incorporate landslides process into the CASCADE landscape evolution model (van de Beek and Braun, 1998). An event-based, momentum-balance method (Lancaster et al., 2003) was used to model mass movement by debris flow in a revised version of the CHILD model. Howard (1998) studied the gully formation and evolution by introducing a 2-D finite-difference model which uses a Lagrangian routing method to track the motion of individual landslides. An upper limit to slope gradient was determined using the simpler variation on this theme to maintain the continuity of mass (Tucker and Slingerland, 1994; Tucker and Bras, 1998). These various event-based methods enable the slope process components of LEMs to have more physically-based mechanisms by making full use of current knowledge of landslides initiation and movement. Although the incorporation of these approaches will likely reduce the computational speed especially for the long-term landscape evolution modelling.

The CL model (Coulthard et al., 2013a) has been used to simulate landscape evolution by calculating erosion and deposition in certain basins and has already been used to simulate sediment movement produced by landslides after a major earthquake (Jun et al., 2018). As previously discussed, there are a wide variety of LEMs, including multi-process catchment models, which apply a holistic view, that provide an effective tool to probe into the impact of internal or external forces on landscape evolution over catchment scale. Among this kind of models, CL has several features giving its precedence compared other catchment models. For example, the incorporation of hydro-dynamic and flow routing process (Lisflood-FP) made it possible for CL to represent the divergent flow which is used to simulate the braided rivers and alluvial formation (Coulthard et al., 2013b), while other catchment models such as SIBERIA, GOLEM and CASCADA commonly apply steepest decent and cascade algorithm to route water across the grid (Coulthard, 2001). Additionally, the spatially distributed rainfall of an hourly rainfall record enables enhanced representation of catchment hydrology (Coulthard et al., 2002), and it can therefore capture the process of discrete storm events that shape landscape evolution. The spatial variations of land use can be also represented by altering the m value in CL (Coulthard and Van De Wiel, 2017), which controls the fluctuation of the soil moisture deficit and thus influences the peak of the modelled flood hydrograph (Coulthard et al., 2002). The spatially distribution of rainfall and land use input allow both temporal and spatial variation of hydrological process in the hydrological model. In CAESAR-Lisflood, sediment is transported as bed load or suspended load for up to nine different grainsize. The selective erosion, and deposition of different grainsizes and transport ways allow a spatially distribution of variable sediment grain size to be simulated. Moreover, the sub-surface sediment data is represented by applying active layers system with a single active layer (the bed load) and multiple buried layers (strata). As a result, changes in grainsize and sediment dynamics can be modelled both vertically and horizontally (Van De Wiel et al., 2007). CL has been applied to research and practice in more than 100 different watersheds around the world. Hancock and others (Hancock, 2012; Hancock and Coulthard, 2012) studied the river channel location evolution and sediment yield law using the CL two-dimensional hydrodynamic landscape evolution model in the Stanley Basin of Australia under different real rainfall scenarios, the results show that the model can well simulate the erosion rate and sediment yield of the river basin and replicate the historical evolution process of the river channel. Coulthard established different land-use change scenarios by changing the “M-value” in the CL model to simulate the connectivity between upstream and downstream sediment yield in the swale basin in northern England (Coulthard and Wiel, 2017). Hancock generated different long-term rainfall sequences randomly and input it to the CL model to simulate the material migration and river channel evolution in the mining area for the first time (Hancock et al., 2017). Meadows (2014) used the CL model to simulate the sediment production and material migration in the downstream watershed after the volcanic eruption in Toutle-Cowlitz basin, US, which also verified the feasibility of simulating the subsequent sediment transport and landform evolution after the disturbance of extreme disaster events. The applications presented indicate the efficiency of CL model to simulate the surface material migration and landscape evolution after anthropogenic and natural disturbances, which indicate the potential to simulate the complexity of surface processes integrated with landslides perturbations.

The rapid development of LEMs provide an alternative and effective way to explore the landslides contribution to the landscape evolution from large spatial scope over a longer term. However, there is no established approach to our knowledge can explicitly track landslide sourced material and thus quantifying the complete role of landslides material to the total sediment budget. Based on the literature review above, the research question is identified - How to investigate the landslide impact on long-term landscape evolution via linking the modelling of sediment transport process and landslide sediment fingerprinting? By integrating an angle threshold of slope failure and tracing function to the CL model, we propose a new modelling approach based CL to investigate the long-term aftermath of landslides on sediment dynamics and landscape evolution.

2. Methods and Model descriptions

2.1 CAESAR-Lisflood

CAESAR-lisflood (CL) is a two-dimensional landscape evolution model (*Figure*) containing a hydrological model, a 2D hydrodynamic flow model, and representations of fluvial erosion and deposition over a range of grainsizes (bed load and suspended) as well as representations of landslides and slope processes (Coulthard et al., 2013a). CL was originally developed to simulate basin hydrology and geomorphology and has become a common tool to simulate and explore geomorphic behavior like erosion and deposition in basins over a range of time and space scales. CL can calculate sediment movement produced by landslides, and replicate the fluvial changes driven by severe rainfall events (Xie et al., 2018), enabling the simulation of the generation and transfer of landslide debris. The core algorithm of CL uses a cellular automaton, the state at each moment is affected by adjacent cells, reflecting the idea that adjacent regions interact with each other in time and space. The model can calculate the flow rate and depth of the corresponding surface runoff according to different rainfall scenarios. Its most prominent function is to be able to delineate the river dynamics (Van De Wiel et al., 2007) and sediment transport process (Coulthard et al., 2002; Shennan et al., 2003) by means of a two-dimensional hydrodynamic model to estimate riverbed erosion and river channel changes (Pelletier, 2004). CL model can also simulate soil creep and slope erosion based on slope angle and different rainfall scenarios (Hancock et al., 2011). Another advantage of CL is that it can simulate over large spatial scales (100 square kilometers) and 1-10000 year time scales, and predict the future riverbed changes and landform evolution.

In the model, the study area is divided into a series of rectangular cells of uniform size (*Figure*). For each grid, the values of properties (e.g. the elevation, vegetation condition, particle size distribution, discharge, water depth, and flow rate. etc.) are stored. During the running of the model, the values stored in each grid are iteratively updated in real time through a series of rules and algorithms based on the surrounding adjacent grids. These calculation rules include four main modules: (1) hydrological module; (2) hydraulic module; (3) erosion and deposition module; (4) slope module; The detailed description of CL can be found in Van De Wiel et al. (2007) and Coulthard et al. (2013b).

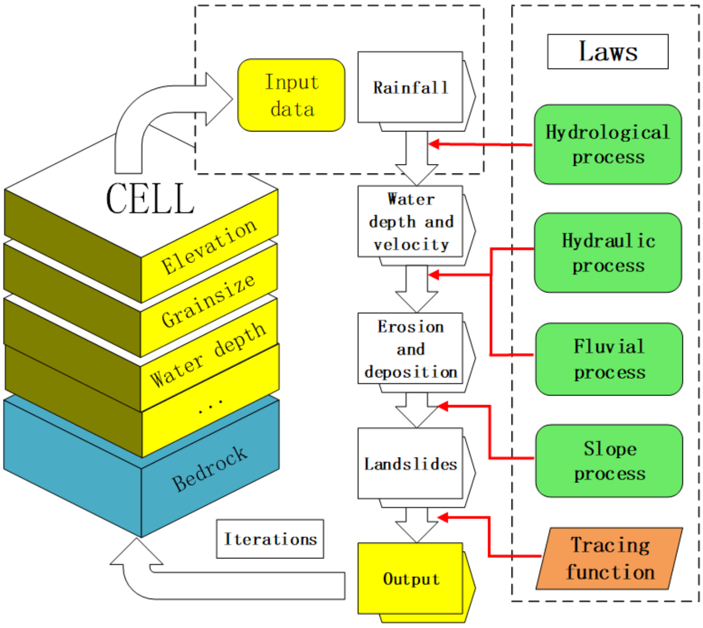

Figure 1. Schematic diagram of CAESAR-Lisflood.

CL can also use spatially distributed rainfall of an hourly record enabling enhanced representation of basin hydrology (Coulthard et al., 2002), and therefore can capture the process of discrete storm events that shape landscape evolution (Coulthard and Skinner, 2016). The spatial variations of land use can be also represented by altering the m value (a parameter control the peak and duration of the hydrograph) in CL (Coulthard and Van De Wiel, 2017), which controls the fluctuation of the soil moisture deficit and thus influences the peak of the modelled flood hydrograph (Coulthard et al., 2002). The spatially distribution of rainfall and land use input allow both temporal and spatial variation of hydrological process in the hydrological model. In CL, sediment is transported as bed load or suspended load for up to nine different grainsizes. The selective erosion, and deposition of different grainsizes and transport ways allow a spatially distribution of variable sediment grainsizes to be simulated. Moreover, the sub-surface sediment data is represented by applying active layer system with a single active layer (the bed load) and multiple buried layers (strata). As a result, changes in grainsize and sediment dynamics can be modelled both vertically and horizontally (Van De Wiel et al., 2007).

2.1.1 Slope process

In CL, slope processes are taken into consideration with 'instantaneous' movement processes such as landslides and slower acting processes such as soil creep (Coulthard et al., 2002). Mass movement such as landslides can be initiated when a user-defined slope threshold angle is exceeded between adjacent cells with material removed from the upper cell and added to the one below to reach the pre-set threshold angle. This process iterates until the angles of all cells affected is lower than the failure threshold. As a small slide in a cell at the base of a slope may trigger more movement uphill, the model continues to check the adjacent cells rows until there is no more movement. Soil creep in hillslope is calculated using a diffusion equation with rates proportional to local slopes between cells.

In the original version of CL (1.9 b), the threshold angle of the mass movement process can be only input as a single global value. This means that the threshold angle within the entire basin is the same, which is not capable to meet the need to investigate the spatial variance of hillslope process or corresponding scenarios. Hence, here we have modified CL model by adding a spatially variable slope failure threshold that is defined by an input file containing the spatial extents of different failure angles. By reducing the failure angle at specific locations we could therefore trigger landslides where required.

2.1.2 Sediment tracing

CL allows for heterogeneous sediment transport, with selective erosion and deposition of up to nine grainsize fractions (Van De Wiel et al., 2007). This provides the potential to keep track of the user defined grain file from a specified source location, thus tracking the transport of sediment from that source area. Specifically, this can be also used to track the landslide generated sediment routing from different source area thus investigate the landslides impact on sediment dynamics and landscape evolution. This tracing functionality builds on that originally developed in the CAESAR model (1997-2011), originally developed for tracking contaminated sediment in rivers from heavy metal mining (Coulthard and Macklin, 2003).

The tracing function in CL is developed by adding another tracer index array to the model, so that the grainsize information of every grid cell is marked with different index to represent different source areas. The grainsize information of each grid cell stores the volume of different size fractions from each of the (assigned) different areas. Therefore, the volume changes and transfers of different size fractions from different source areas can be tracked and traced. The number of source areas can be set up by pre-defining the number of tracers in the tracer index array. There is a computational overhead associated with this modification – as the calculation of erosion and deposition for each cell has to be carried out for the number of source areas. Erosion and deposition components of the model code account for c.70% of model run time – therefore increasing these by a factor of two or greater can significantly increase model run times.

2.2 Model modification

The slope module in CL can simulate the slope instability and soil creep of basin slopes to some extent. However, the model over-simplifies the slope instability process and cannot effectively reflect the spatial heterogeneity of landslide initiation simulation. Moreover, CL cannot track landslide-generated sediment production and its transport, the model output does not distinguish between landslide and non-landslide sediment production, and thus cannot quantify the contribution and quantitative impact of landslides on the total sediment yield in the study basin. For the purpose of this study, based on CL model, by modifying the landslide triggering in slope module and adding the sediment (material) transport tracing function to the model, we are able to incorporate the triggering of landslides and the sediment transport tracing of landslide generated material. *Figure* shows the workflow diagram of the model modification for spatial-heterogeneously landslide triggering and subsequent landslide-generated sediment transport tracing based on CL model. The model version modified here was CAESAR-Lisflood 1.9j.

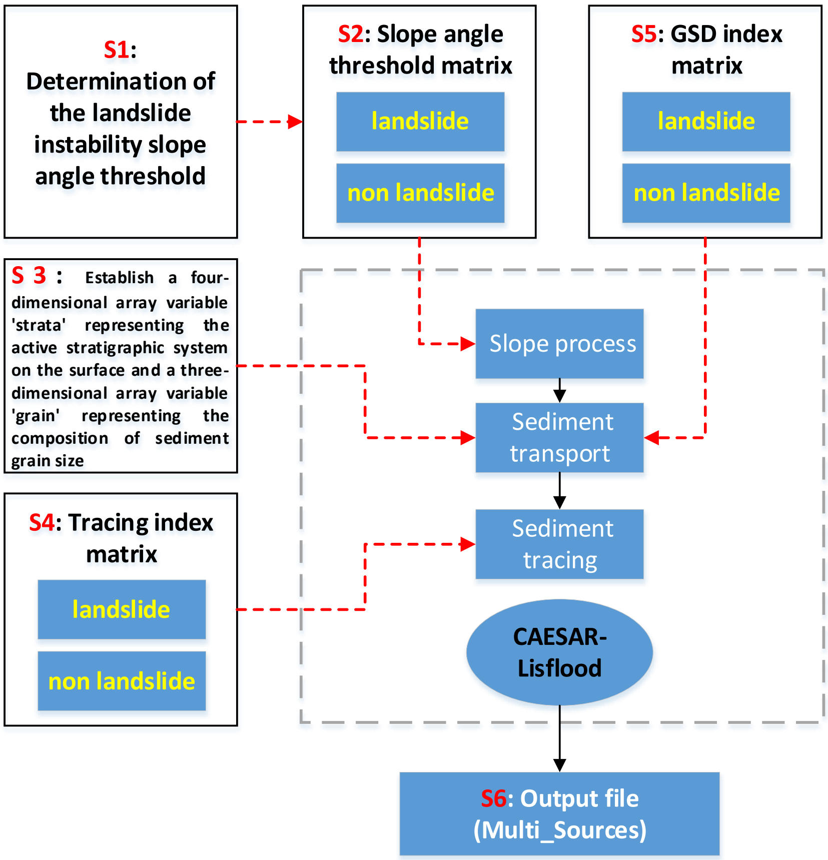

Figure 2. Schematic diagram of landslide-derived sediment tracing in CL

The detailed description of the tracing process of landslide-derived sediment transport are illustrated below.

S1: The geological, geomorphological, and hydrological factors of the basin can be combined to determine the landslide failure angle threshold of the basin (Freeze, 1987). For example, geomorphological and hydrological factors including soil cover characteristics, geological rock types, rock structure, earth surface slope, and groundwater distribution can pose a critical role in the slope stability. These factors can be obtained through field investigation, available historical documentation, etc. The landslide failure angle threshold can be calculated using safety-of-factor index method based on these controlling factors. Additionally, using statistical method based on historical seismic-landslide inventory can also estimate the landslide failure angle threshold, which can be determined by those skilled experts according to the specific conditions of different basins/areas.

S2: By calculating the slope failure angle thresholds at different locations, a spatial distribution file of slope failure angle threshold across the basin is established. A spatial index for each grid cell is used to establish a spatial link between the slope threshold distribution file with other dataset used in the CL model.

This spatial distribution file, i.e., the two-dimensional slope angle threshold index file is a two-dimensional matrix that corresponds to the spatial extent and resolution of the basin DEM (Digital Elevation Model) file, and each matrix element stores the slope failure angle threshold at the corresponding location. The index file name with file suffix is entered by adding a text input box to the slope module of the model GUI interface. When the model reads the file and initializes, the index file is written to the model and converted into a two-dimensional matrix, and the slope failure angle thresholds are linked to other model data (e.g., topographic data, which are used to calculate watershed slope angles) through the spatial index, thus calculate where the landslide could occur and the amount of material moved.

S3: Based on the CL model, a four-dimensional array variable *"strata [xyindex, z, n, T]"* representing the active stratigraphic strata layer system on the surface and a three-dimensional array variable *"grain [xyindex, n, T]"* representing the composition of sediment grain size were established, where *"xyindex"* represents the spatial index, *z* stores the stratigraphic index, taking values in the range of 1-10 , representing 10 active strata layers; *n* stores the corresponding sediment grain size fraction index, taking values in the range of 1-9, representing 9 different sediment grain size ranges, *T* represents the trace index value (described in **S4** below), taking values in the range of 1-m, m is the predefined number of trace index values, a natural number greater than 1, representing m different material source areas.

More specifically, the CL model represents the surface sediment (material) composition by creating an active stratigraphic system (*strata*). The active stratigraphic system consists of an uppermost top active stratum, multiple lower active strata, and a bedrock layer. The model is able to define up to 9 different particle sizes for each active stratum, and the model user can set the number of particle sizes and the value of the grain size range according to the specific situation. The model also uses a sediment composition variable (*grain*) to store the proportion of the volume of the nine different grain sizes in the corresponding stratigraphic volume, which is used to quantify the amount of sediment of different grain sizes at different basin locations and the subsequent transport. The model simulates the results of sediment transport at different locations in the basin by iteratively computing the stratigraphic system (*strata*) and the corresponding sediment (*grain*) composition, and then calculates the amount of topographic variation and sediment production in the basin. The stratigraphic layer system and sediment grain composition are defined as "*strata*" and "*grain*" respectively.

S4: A two-dimensional sediment source index matrix is established (*Figure 3*), the spatial extent corresponding to different sediment source zones are initially defined. It is then input to the CL model and integrated into the modelling process via a spatial index.

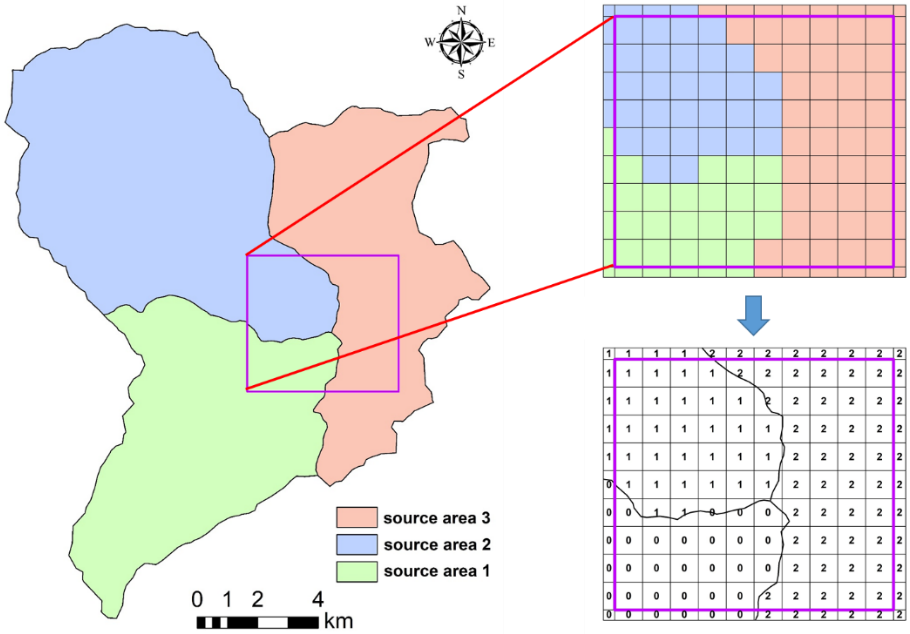

Figure 3. Schematic diagram of tracer index matrix derived from source areas

More specifically, the number of material source tracking indexes, m, can be predefined to represent m different material source areas. A two-dimensional matrix file with the same area range and spatial resolution as the DEM (Digital Elevation Model) file is then created (the number of indexes can be customized; if the material source is divided into landslide and non-landslide areas only, the number of indexes is 2 and the tagged index values are 1 and 2; if three material source areas are defined, the number of indexes is 3 and the tagged index values are 1, 2 and 3; and so on). By adding two input text boxes to the GUI interface of CL model, one for entering the number of predefined indexes and one for entering the file name of the tracing index file with the file suffix. When the model reads the file and initializes, the trace index file is written to the model and converted into a two-dimensional matrix, where each value of the matrix is tagged with the index value of the material source at that location, and the tracer index value are assigned to the value of *"T"* in *"strata [xyindex, z, n, T]"* and *"grain [xyindex, n, T]"*, respectively. The number of matrix index values corresponds to the number of predefined material source trace indexes *m*.

S5: A spatial index matrix file of grain size distribution (GSD) in the basin is established (*Figure 4*), and each index corresponds to a specific particle size distribution input to CL model. This GSD index file is used to establish a spatial link between other dataset used in the CL model and the sediment GSD via spatial index described above.

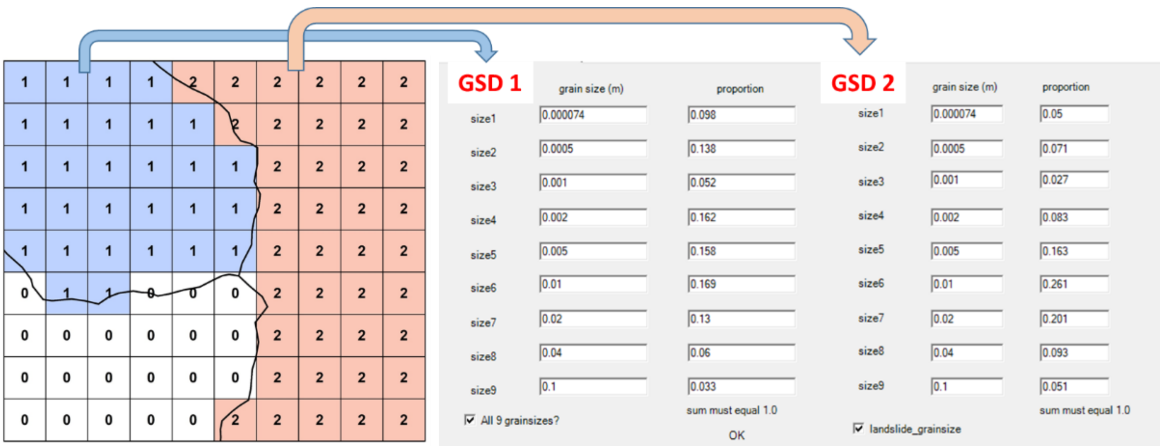

Figure 4. Schematic diagram of GSD index matrix

In previous versions of CL the initial input of sediment GSD was global. Most previous studies of CL had used a lumped GSD input for the whole basin where each grid cell of the basin have the same GSD of sediment, under which case the CL needs to adjust the grain size distribution across the basin via preconditioning runs known as spinning up. Prior to undertaking the forecasting simulations, spinning up is necessary to define the initial conditions for grain size and topography. This enables the model to flush fine sediment from the in-channel cells and remove any small perturbations in the initial DEM that may lead to excessively high initial sediment yields. Also, there is a toolbox to generate grain input file (up to 6 different GSD) for CL with spatially variation of initial sediment GSD for each grid cell. There have been some recent studies applying it to study the impact of spatially variation of particle size on sediment dynamics in a post-mining landscape (Hancock et al., 2020). However, here, we attempt to investigate the impact of spatial heterogeneity of sediment GSD and trace the routing of landslide generated sediment transport. The grain input file is not applicable due to the addition of dimension of grainsize variable – *"grain"* to enable the tracing function (described above). We thus modify the model so the different GSD can be input via spatially fixed pre-determined areas, this is achieved by an index matrix with each index corresponding to one specific area where there has the same sediment GSD input.

S6: The modified CL model can then be used to initiate the landslide occurrence with different GSD inputs and calculate the sediment transport of each tracing source area thus track the sediment dynamics from different material source areas including landslides affected region. The refined CL model can output a series of simulation results, which includes the daily sediment yield from each material source area with up to nine grain size fraction (total or separate) at the basin outlet and the spatial distribution of sediment transport of each material source as well as the elevation change for the whole basin or local landform change at user-defined time interval.

More specifically, the CL model reads the spatial distribution file of landslide slope angle thresholds in the basin, calculates the extent of the slope instability area and triggers the landslide, and calculates the material transfer due to the occurrence of the landslide. Based on the two-dimensional index matrix, the corresponding slope instability angle thresholds are obtained for each location. At each location, based on DEM (Digital Elevation Model) in each model run step, the slope angle is compared with the slope instability angle threshold at the corresponding location. If the slope angle at that location is less than the unstable slope angle threshold, the slope at the location is regarded as a stable condition and no landslide occurs.

If the slope angle at the location is greater than the unstable slope angle threshold, the landslide is triggered. The process is repeated iteratively until the slope angle in each area of the basin is less than or equal to the instability slope angle threshold. Then, based on the slope process and sediment transport process of the CL model, and using the two-dimensional sediment tracing index matrix we can simulate and track the sediment transport process from different material source areas.

2.3 Model configuration

A 95-yr simulation was conducted using the modified CL model with the tracing function to provide an example of the refined capability of the CL model to track the sediment transport process derived from different source areas. Acknowledging uncertainty in the model parameter evaluation, the aim of this study was not to replicate the observed occurrence of landslides as accurately as possible with one simulation, but to demonstrate of the ability of the revised CL model to track the landslide sediment dynamics thus investigating spatial-temporal pattern of sediment transport with several assumptions.

The study area of this demonstration was Hongxi river basin, located in Pingwu district, Sichuan province, southwestern China, with a watershed area of 179 km^2. A total of 233 landslides were triggered in the study area during the Wenchuan earthquake (Fig.1c). Due to the differences in location and topography of landslides, there are clear differences in morphology and scale characteristics between landslides. Over 75% of the landslide inventory is located in the downstream basin, three (Wenjiaba, Zhenjiashan and Shanxingqu) of the four largest landslides of the study area are located in downstream and one (Maanshi) in upstream. The model parameters used in this study are listed in Table 1. The detailed description of model parameters and set up can be found in https://sourceforge.net/p/caesar-lisflood/wiki/Tab%20Parameters%20%28description%20of%20model%20parameters%29/.

Table 1 Model parameters description

Parameters	Values	Description of parameter
Grain sizes (m)	0.000074, 0.0005, 0.001, 0.002, 0.005, 0.01, 0.02, 0.04, 0.1	Used for sediment transporting calculation in each active layer
Grain size proportions	0.098, 0.138, 0.052, 0.162, 0.158, 0.169, 0.13, 0.06, 0.033	Denotes the fractional volume of the grain-size in each active layer
M value	0.003 for landslide and 0.02 for no landslide area	Controls the peak and duration of the hydrograph generated by a rain event. It is the same as the 'm' value in TOPMODEL
Min Q/Max Q	0.5/5	Min Q is a threshold above which CL will calculate a flow depth, Max Q is the maximum discharge to be added to a cell
Sediment transport law	Wilcock and Crowe equations	Works with multiple grain sizes across the sand and gravel range
Max erode limit (m)	0.02	The maximum amount of material that can be eroded or deposited within a cell at each time step
Active layer thickness (m)	0.2	The thickness of a single active layer
Lateral erosion rate	0.000001	The variable controls lateral erosion
Soil creep/diffusion value	0.025	The variable that forms part of the USLE equation
Courant number	0.7	The value controls the numerical stability and speed of operation of the flow model
Manning's n	0.04	The roughness co-efficient used by the flow model

Tracer index delineation

To demonstrate the functions associated with the sediment tracing module, four largest landslides trigged by the 2008 Wenchuan earthquake in the study basin were selected as the source areas of landslides to be tracked. The domain of each individual landslide and non-landslide area were then converted to grid format with 50 m *50 m resolution at Arcmap 10.6 platform (Fig. 5). Five tracer index were generated and input to the CL model to track the different sourced sediment transport and dynamics. The area without landslide impact (background area) is marked with tracer index 0, each of the top 4 largest landslides was marked with a single tracer index (1-4) respectively corresponding to different source areas.

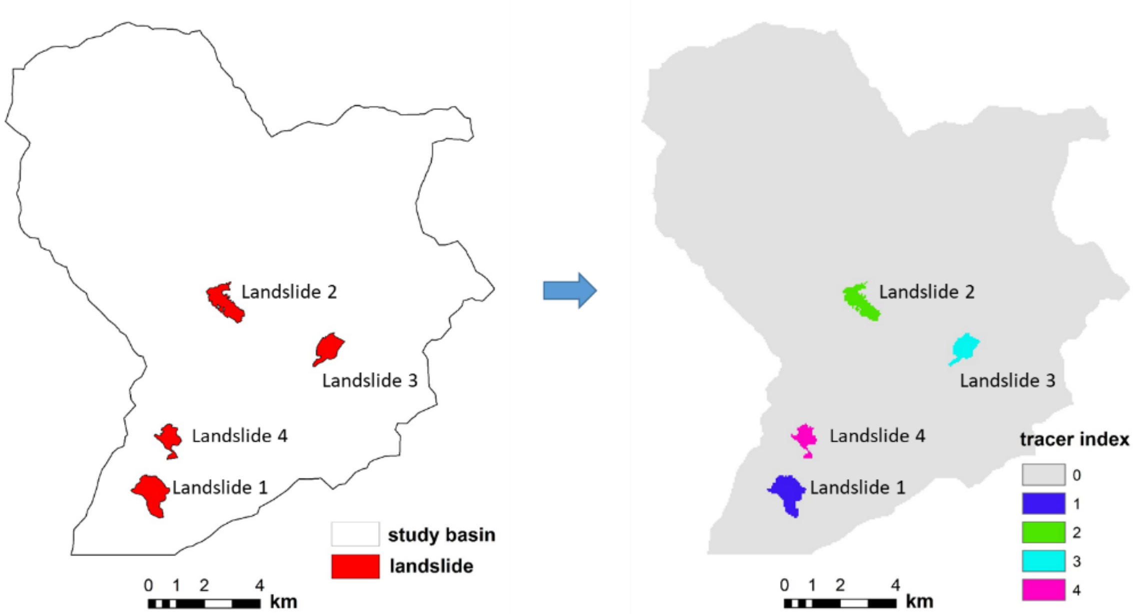

Figure 5. Main landslides and Tracing index delineation

3. Results

The modelling results (figure 6) shows that the landslides can move substantial hillslope material into lower slope and transport into downstream channel. The elevation changes after decades of simulation clearly present the spatial pattern of erosion and deposition. At the beginning of the simulation, the landslides are triggered via slope angle threshold (figure 6a). 'Instantaneous' movement of hillslope material caused drastic erosion at the landslide domain, the displaced material deposit at the lower part of the hillslope. The landslide generated sediment then further transport along the main channel. The elevation changes at the end of the simulation (figure 6b) show that the erosion mainly occur in headwater channels apart from the landslide affected area. It should be also noted that there are significant sediment accumulation in the main channel downstream of the basin due to the sediment transport from headwater channel and landslides sources.

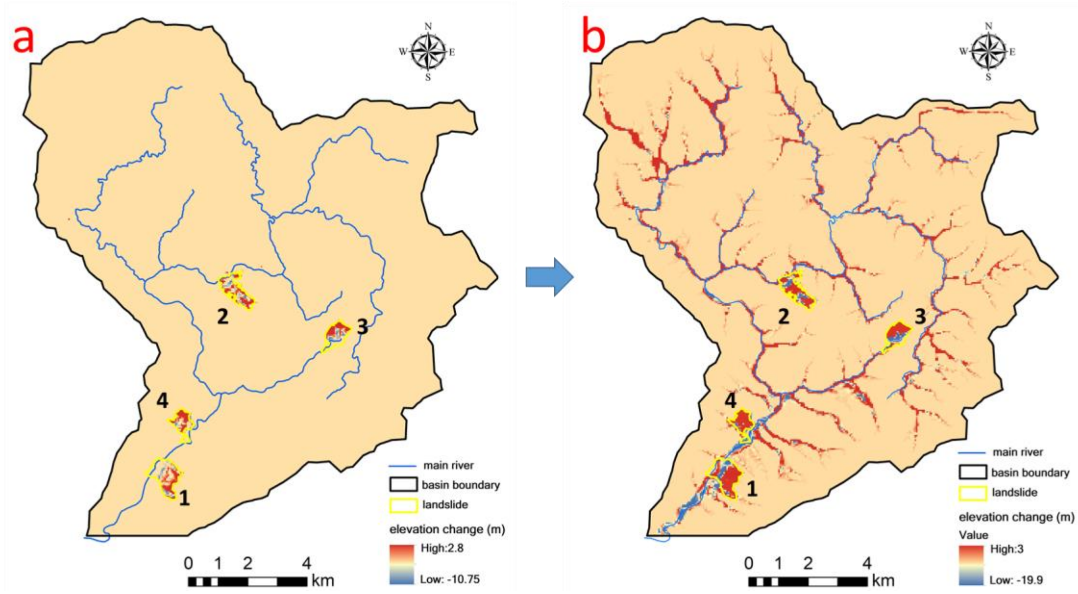

Figure 6. Spatial pattern of elevation changes a) at the beginning of the simulation b) at the end of the simulation. For elevation changes, positive value denote erosion and negative value denote deposition.

The modified version of CL can also output the spatial pattern of sediment transport for each sourced area or landslide (figure 7a), which enable to track the landslide sediment transport and dynamics. Using these output files we can quantitatively analyse the spatial and vertical distribution of tracked sediment. Figure 7b shows the route and extent of landslide-sourced sediment transport, which can be processed to generate the longitudinal profile of deposition thickness for specific sourced sediment (Figure 7c).

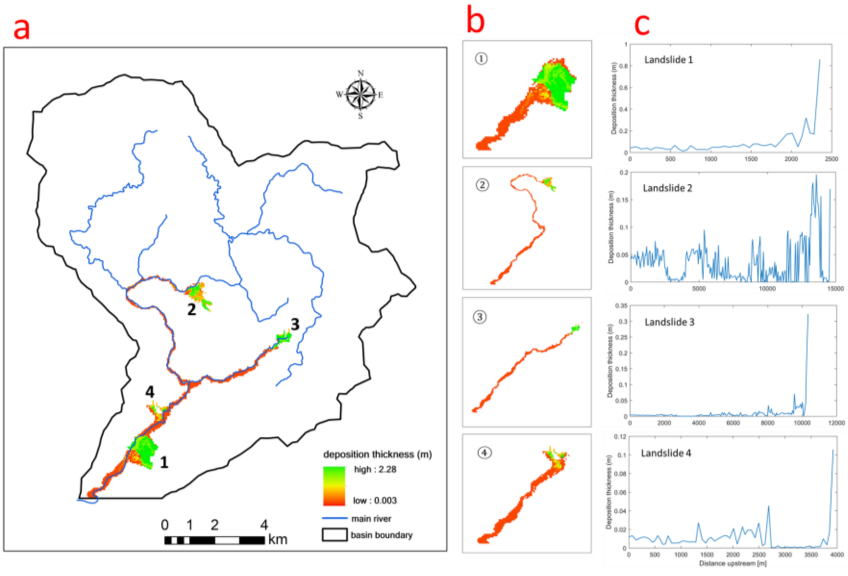

Figure 7. Landslide-sourced sediment tracing. a) Spatial pattern of landslide sediment transport. b) Fingerprint of individual landslide-sourced sediment. C) Longitudinal profile of landslide sediment deposition along flow path.

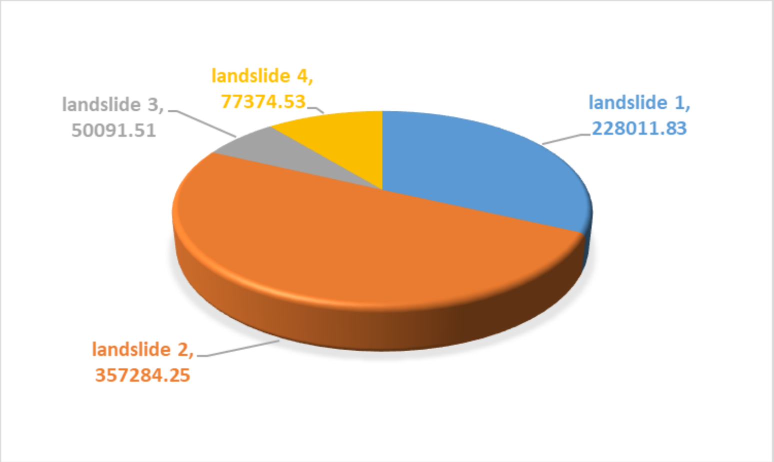

Figure 8. Landslide-sourced sediment yield (m^3) at the basin outlet

The modified CL enable us to generate the sediment yield from each traced individual landslide. The landslide tracked sediment yields (Figure 8) shows that the landslide 2 has the highest sediment yield followed by landslide 1 and landslide 4 with landslide 3 presenting the least amount sediment yield. It's noteworthy that the sediment yield of landslide 2 constitute almost half of the total landslide sediment yield.

4. Discussion

In this study, an approach using a spatially variable slope threshold was firstly applied in CL. The simulation results indicate that the modified CL can represent landslides occurring where assigned from a real landslide inventory according to the failure angle threshold (figure 6). This provide potential to investigate the aftermath of seismic landslides including its immediate (figure 6a) and long-term (figure 6b) impacts on landform evolution. There is growing evidence that landslides can not only exerts direct impact on the landforms by removing mass material from hillslope but also have a long term impact on fluvial processes (Korup et al., 2010). It's clearly shown from figure 6b that landslide-derived sediment transport can pose off-site impacts on basin geomorphic changes especially for the downstream main channel. Significant accumulation has occurred in the lower part of the main channel of the basin and landslides largely dominate the erosion on hillslopes. This was also reported by Yang et al. (2015) that there is substantial deposition on the downstream river channel leading to the rising and broadening of the river morphology in this study area. The study of Xie et al. (2022b) also shows that landslides can have huge impacts on landforms not only in landslide affected regions or nearby but the far downstream channel.

Quantifying the amount of landslide related sediment budget and time-scale of the long-term legacy of seismic landslides is crucial to understand the complete role of landslides on the sediment dynamics and landform changes. However, the quantification of landslide-sourced sediment dynamics and routing remains an open question (Tsai et al., 2013). A modified version of CL model was firstly developed with a tracing function integrated to investigate quantitatively the landslide impact on landscape evolution. The simulation results of this study (figure 7) show that the modified CL can generate not only the spatial pattern but also the vertical thickness of sediment transport from each sourced area. Moreover, the model can also output the sediment yield at the basin outlet from different sourced areas. All these model output can be generated at user specified time interval. This enable us to investigate the landslide-generated sediment dynamics and its impact on landscape evolution over a broad scales of time and space. Specifically, the landslide 2 in our simulation presents the highest sediment yield and landslide 3 has the least sediment yield, which indicates that landslide-sourced sediment yield is not entirely dependent on the size of the landslide. The landslide sediment yield might be determined by a combination of intrinsic and extrinsic factors including landslide location, local landforms and meteorological factors. Xie et al. (2022a) found the location of landslides can affect the landslide-channel connectivity, thus altering the sediment yields and spatial pattern of sediment dynamics. Further, Xie et al. (2022b) used the CL integrated tracing function to determine the role of landslide-sourced sediment to the total sediment budget from three sub-basins, which shows that the contribution of landslides is dependent on the landslide area density of specific basin.

The ability to trace the sediment dynamics (both bed load and suspended sediment) sourced from individual landslides is an important addition to our modelling capability with many possible uses. As previously described, for the modelling aims, we mainly focus on the sediment transport after the landslide occurring rather than the prediction of landslides occurring. Therefore, every landslide location is determined before the simulation using a failure angle threshold which is derived from the real landslides inventory. The landslides simulated in the CL model are not generated by simulated earthquakes. Also, we do not consider the evolution of new landslides occurring during the modelling process although any slope steepening due to erosion (for example) will lead to smaller landslides during the simulations. The dynamic landslides prediction and triggering mechanism (earthquake and rainfall) coupled with other module of CL including hydrological and fluvial process should be further investigated and remains an aspiration for future research. Additionally, the combination and partitioning between rainfall and earthquake triggered landslides is also an open question when integrated to LEM simulations. In terms of sediment tracing, here, we use a basic version of the tracing feature to look at the transport and fate of sediment from a single set of landslides, but future model developments aim to allow the tracking of individual landslides within a large grouping to better understand the dynamics of landslide sourced sediment transport. Therefore, this approach applied in CL here is supposed to be extended and improved using more robust and reliable modelling framework with more physically-based mechanisms to offer more in-depth insight in post-earthquake risk assessments and mitigations.

5. Conclusions

A number of modifications made to the CL are the first attempts to use numerical simulation models to combine slope disturbances within long-term basin landform changes and sediment dynamics, exploring the possibility and feasibility of using numerical models to quantify the long-term impact of landslides on sediment dynamics and landscape evolution.

Modified CL can generate not only the spatial pattern but also the vertical extent of sediment transport from each sourced area. The model can generate the sediment yield at the basin outlet from different sourced areas at user specified time interval. This enable us to investigate the landslide-generated sediment transport and fingerprinting over a broad scales of time and space.

The modelling results indicate that the landslides can change the landform a lot immediately after their occurring and exert off-site influence on the geometry of downstream channel in the long term. The landslides will facilitate the transfer rate of material from hillslope to the fluvial channel and exported out of the basin thus playing an important role on the basin landscape evolution.

Acknowledgements

This research work is a part of the doctoral research supported by the joint scholarship program provided by China Scholarships Council (No.201806040215) and the University of Hull. The CAESAR-Lisflood model is freely available from https://sourceforge.net/projects/caesar-lisflood/files/.

References

Armitage, J.J., Allen, P.A., Burgess, P.M., Hampson, G.J., Whittaker, A.C., Duller, R.A., Michael, N.A., 2015. Sediment Transport Model For the Eocene Escanilla Sediment-Routing System: Implications For the Uniqueness of Sequence Stratigraphic ArchitecturesSEDIMENT TRANSPORT MODEL FOR THE EOCENE ESCANILLA. Journal of Sedimentary Research, 85(12), 1510-1524.

Cendrero, A., Dramis, F., 1996. The contribution of landslides to landscape evolution in Europe. Geomorphology, 15(3-4), 191-211.

Claessens, L., Lowe, D.J., Hayward, B., Schaap, B., Schoorl, J., Veldkamp, A., 2006. Reconstructing high-magnitude/low-frequency landslide events based on soil redistribution modelling and a Late-Holocene sediment record from New Zealand. Geomorphology, 74(1-4), 29-49.

Coulthard, T., Macklin, M., Kirkby, M., 2002. A cellular model of Holocene upland river basin and alluvial fan evolution. Earth Surface Processes and Landforms, 27(3), 269-288.

Coulthard, T.J., 2001. Landscape evolution models: a software review. Hydrological processes, 15(1), 165-173.

Coulthard, T.J., Macklin, M.G., 2003. Modeling long-term contamination in river systems from historical metal mining. Geology, 31(5), 451-454.

Coulthard, T.J., Neal, J.C., Bates, P.D., Ramirez, J., Almeida, G.A.M.D., Hancock, G.R., 2013a. Integrating the LISFLOOD‐FP 2D hydrodynamic model with the CAESAR model: implications for modelling landscape evolution. Earth Surface Processes & Landforms, 38(15), 1897-1906.

Coulthard, T.J., Neal, J.C., Bates, P.D., Ramirez, J., de Almeida, G.A., Hancock, G.R., 2013b. Integrating the LISFLOOD‐FP 2D hydrodynamic model with the CAESAR model: implications for modelling landscape evolution. Earth Surface Processes and Landforms, 38(15), 1897-1906.

Coulthard, T.J., Skinner, C.J., 2016. The sensitivity of landscape evolution models to spatial and temporal rainfall resolution. Earth surface dynamics, 4(3), 757.

Coulthard, T.J., Van De Wiel, M.J., 2017. Modelling long term basin scale sediment connectivity, driven by spatial land use changes. Geomorphology, 277, 265-281.

Coulthard, T.J., Wiel, M.J.V.D., 2017. Modelling long term basin scale sediment connectivity, driven by spatial land use changes. Geomorphology, 277, 265-281.

Densmore, A.L., Ellis, M.A., Anderson, R.S., 1998. Landsliding and the evolution of normal‐fault‐bounded mountains. Journal of geophysical research: solid earth, 103(B7), 15203-15219.

Freeze, R., 1987. Modelling interrelationships between climate, hydrology, and hydrogeology and the development of slopes. Slope Stability: Geotechnical Engineering and Geomorphology. John Wiley and Sons New York. 1987. p 381-403, 10 fig 2 tab, 30 ref.

García-Castellanos, D., Cloetingh, S., Busby, C., Azor, A., 2012. Modeling the interaction between lithospheric and surface processes in foreland basins. Tectonics of Sedimentary Basins: Recent Advances, 152-181.

Hancock, G., 2012. Modelling stream sediment concentration: An assessment of enhanced rainfall and storm frequency. Journal of hydrology, 430, 1-12.

Hancock, G., Coulthard, T., 2012. Channel movement and erosion response to rainfall variability in southeast Australia. Hydrological Processes, 26(5), 663-673.

Hancock, G., Coulthard, T., Martinez, C., Kalma, J., 2011. An evaluation of landscape evolution models to simulate decadal and centennial scale soil erosion in grassland catchments. Journal of hydrology, 398(3-4), 171-183.

Hancock, G., Saynor, M., Lowry, J., Erskine, W., 2020. How to account for particle size effects in a landscape evolution model when there is a wide range of particle sizes. Environmental Modelling & Software, 124, 104582.

Hancock, G., Verdon-Kidd, D., Lowry, J., 2017. Sediment output from a post-mining catchment–Centennial impacts using stochastically generated rainfall. Journal of hydrology, 544, 180-194.

Howard, A.D., 1998. Long profile development of bedrock channels: Interaction of weathering, mass wasting, bed erosion, and sediment transport. Geophysical Monograph-American Geophysical Union, 107, 297-319.

Jun, X., Ming, W., Kai, L., Coulthard, T.J., 2018. Modeling sediment movement and channel response to rainfall variability after a major earthquake. Geomorphology.

Kirkby, M., 1984. MODELING CLIFF DEVELOPMENT IN SOUTH-WALES-SAVIGEAR RE-VIEWED. Zeitschrift fur Geomorphologie, 28(4), 405-426.

Korup, O., 2009. Linking landslides, hillslope erosion, and landscape evolution. Earth Surface Processes and Landforms, 34(9), 1315-1317.

Korup, O., Clague, J.J., Hermanns, R.L., Hewitt, K., Strom, A.L., Weidinger, J.T., 2007. Giant landslides, topography, and erosion. Earth and Planetary Science Letters, 261(3-4), 578-589.

Korup, O., Densmore, A.L., Schlunegger, F., 2010. The role of landslides in mountain range evolution. Geomorphology, 120(1-2), 77-90.

Lancaster, S.T., Hayes, S.K., Grant, G.E., 2003. Effects of wood on debris flow runout in small mountain watersheds. Water Resources Research, 39(6).

Meadows, T., 2014. Forecasting long-term sediment yield from the upper North Fork Toutle River, Mount St. Helens, USA, University of Nottingham.

Pelletier, J.D., 2004. Persistent drainage migration in a numerical landscape evolution model. Geophysical Research Letters, 31(20).

Shennan, I., Coulthard, T., Flather, R., Horton, B., Macklin, M., Rees, J., Wright, M., 2003. Integration of shelf evolution and river basin models to simulate Holocene sediment dynamics of the Humber Estuary during periods of sea-level change and variations in catchment sediment supply. Science of the total environment, 314, 737-754.

Tsai, Z.X., You, G.J.Y., Lee, H.Y., Chiu, Y.J., 2013. Modeling the sediment yield from landslides in the Shihmen Reservoir watershed, Taiwan. Earth Surface Processes and Landforms, 38(7), 661-674.

Tucker, G., Lancaster, S., Gasparini, N., Bras, R., 2001. The channel-hillslope integrated landscape development model (CHILD), Landscape erosion and evolution modeling. Springer, pp. 349-388.

Tucker, G.E., Bras, R.L., 1998. Hillslope processes, drainage density, and landscape morphology. Water Resources Research, 34(10), 2751-2764.

Tucker, G.E., Hancock, G.R., 2010. Modelling landscape evolution. Earth Surface Processes and Landforms, 35(1), 28-50.

Tucker, G.E., Slingerland, R.L., 1994. Erosional dynamics, flexural isostasy, and long-lived escarpments: A numerical modeling study. Journal of Geophysical Research: Solid Earth, 99(B6), 12229-12243.

van de Beek, P., Braun, J., 1998. Numerical modelling of landscape evolution on geological time-scales: A parameter analysis and comparison with the south-eastern highlands of Australia. Basin Research, 10(1), 49-68.

Van De Wiel, M.J., Coulthard, T.J., Macklin, M.G., Lewin, J., 2007. Embedding reach-scale fluvial dynamics within the CAESAR cellular automaton landscape evolution model. Geomorphology, 90(3-4), 283-301.

Veldkamp, A., Van Dijke, J., 2000. Simulating internal and external controls on fluvial terrace stratigraphy: a qualitative comparison with the Maas record. Geomorphology, 33(3-4), 225-236.

Xie, J., Coulthard, T.J., McLelland, S.J., 2022a. Modelling the impact of seismic triggered landslide location on basin sediment yield, dynamics and connectivity. Geomorphology, 398, 108029.

Xie, J., Coulthard, T.J., Wang, M., Wu, J., 2022b. Tracing seismic landslide-derived sediment dynamics in response to climate change. CATENA, 217, 106495.

Xie, J., Wang, M., Liu, K., Coulthard, T.J., 2018. Modeling sediment movement and channel response to rainfall variability after a major earthquake. Geomorphology, 320, 18-32.

Yang, W., Wang, M., Kerle, N., Van Westen, C., Liu, L., Shi, P., 2015. Analysis of changes in post-seismic landslide distribution and its effect on building reconstruction. Natural hazards and earth system sciences, 15(4), 817-825.